

Modeling and processing of SAR images

Nikita Andriyanov

JSC "RPC "Istok" named after Shokin
Fryazino, Moscow Region, Russia;
Telecommunication department
Ulyanovsk State Technical University
Ulyanovsk, Russia
nikita-and-nov@mail.ru

Danila Andriyanov

Telecommunication department
Ulyanovsk State Technical University
Ulyanovsk, Russia
boss.renome@mail.ru

Abstract—The text is devoted to the method of simulating radar images based on harmonic analysis. The possibilities of impelenting small and distributed objects in the coordinates of inclined and track ranges are considered. Moreover, for a number of reference objects, a detection algorithm based on the Neyman–Pearson criterion was implemented and investigated, and an algorithm for recognizing reference targets was also proposed.

Keywords—SAR images; radar images; object detection; image processing

I. INTRODUCTION

The processing of Earth remote sensing data is of particular interest these days. Moreover, such data is usually represented by multidimensional arrays of information. Today there are a lot widespread methods for processing satellite images based on mathematical models of random fields (RF) [1-4] and machine learning methods [5-7]. Indeed, in the course of such processing a number of applied problems are solved. In particular, the work [1] is devoted to methods of filtering and reconstructing satellite images based on doubly stochastic models. The work [2] describes a method of image segmentation, which in combination with other segmentation algorithms can improve the quality of segmentation. A wide study of methods for processing satellite images using doubly stochastic models is presented in [3]. In addition to doubly stochastic models, models based on autoregressions with multiple roots of characteristic equations were proposed for describing and processing images providing lower computational costs [4].

However, mainly in the literature on image processing, authors are talking about processing two-dimensional brightness fields in grayscale or two-dimensional brightness fields in several color channels. This refers to optical images. However, despite the wide distribution, such images have some drawbacks. One of them is the dependence of the work of registrars on weather conditions. Clouds and other disturbing natural factors can often be found in images. In order to register the Earth's surface regardless of weather conditions, synthetic aperture radar (SAR) can be used, the result of which are radar images (SAR images) [8-11]. By and large, such images also represent a two-dimensional array of brightness elements, however, the method of their formation is of interest. It is close to processing of multichannel data [12]. Radar images and it's processing are considered in [13-16]. The main attention of such data processing is devoted to tasks of modeling and objects recognition. New modeling methods was suggested [16], however in the number of task it is expedient to use classical models of SAR. In this paper, an example of modeling radar images and objects on its background are considered. The

detection characteristics of small point objects is also investigated.

II. SYNTHETIC APERTURE RADARS

The quality of radar images is characterized by their resolution. To determine the linear resolution in azimuth, it is possible to use the expression

$$\delta x = \theta_A r = r \lambda / d_A, \quad (1)$$

where θ_A is a horizontal beamwidth of the antenna, r is a slant range, λ is wavelength, d_A is horizontal aperture size of the antenna.

Spatial resolution on slope δr and horizontal range resolution δy determined respectively by the duration of the probe pulse τ_u and viewing angle (observation angle) γ

$$\delta r = \frac{c \tau_u}{2}, \delta y = \delta r \sec \gamma, \quad (2)$$

where c is speed of light.

An analysis of expressions (1) and (2) shows that it is possible to improve the resolution by increasing the size of the aperture of the antenna and reducing the duration of the probe pulses. However, in the second case, the energy of the probe signal decreases, and with it the observation range. The horizontal size of the antenna is limited by the size of the aircraft from which the sounding is performed. Therefore, the parameter d_A is artificially enlarged by synthesizing the image along the route of the aircraft. And such systems are called SAR stations.

III. MATHEMATICAL MODEL OF THE PROCESS OF FORMING SAR IMAGES

For adequate modeling of the radar image formation process, it is necessary to simulate a number of processes and factors important for the formation of such an image. In [9] it was proposed to use the following models:

1) Model of reflection (scattering) of an electromagnetic wave (EMW) by the Earth (sea) surface and objects. Let such a model be described by the operator L_{pp} .

2) Model for generating a radar signal, including 2 procedures: conversion of the electromagnetic field (EMF) scattered by the observed surface, described by the remote sensing operator L_s , and a procedure for scanning an EMF having two-dimensional coordinates into a one-dimensional

radar signal. The last procedure is described by the spatio-temporal scan operator L_{nec} .

3) Model of noise and interfering factors, for the description of which the distortion operator L_u is used.

4) Model for processing the complex envelope of the signal and the formation of radar data, which, as well as the model for generating the radar signal, is represented by two procedures such as the data processing procedure itself and the procedure for converting the radar signal into an image. The first is described by the processing operator L_{obp} , the second is described by the operator L_{nec}^{-1} , the inverse of the spatial-temporal scan operator.

Thus, according to [9], to describe the mathematical model of radar data, 6 operators and the radar terrain function (RTF) are used. RTF can be written as follows

$$\hat{e}(r, x) = e(r, x) \exp[j \psi(r, x)], \quad (3)$$

where $e(r, x)$ and $\psi(r, x)$ are amplitude and phase characteristics of scattered EMF.

Fig. 1 shows the radar image of a point object.

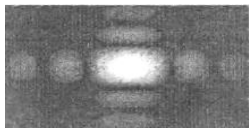


Fig. 1. SAR image with point object.

It should be noted that not only the point object itself is clearly visible in the image, but also the area in the point object neighborhood.

IV. RADAR IMAGES MODELING BY HARMONIC ANALYSIS

Let the path signal $\hat{s}(m, n)$ is signal reflected along the m -th strip of range. Then it represents the sum of signals from elementary reflectors $\hat{s}_i(m, n)$. Passing to continuous time, it is possible to write the following equation

$$\begin{aligned} \hat{s}_{mi}(t) &= U_i G(t - t_i) \exp\{-j[\alpha(t - t_i)^2 - \varphi_{oi}]\} =, \\ &= U_i G(t - t_i) \exp\{-j\alpha t^2\} \exp\{j(\omega_{oi} t + \varphi_i)\} \end{aligned} \quad (4)$$

where $U_i G(t - t_i)$ is signal envelope determined by the shape of the antenna pattern in the azimuthal plane,

$$\alpha = \frac{2\pi V_n^2}{\lambda r_0}, \quad r_m \leq r_0 < r_m + \Delta r,$$

$$\omega_{oi} = \frac{4\pi V_n^2 t_i}{\lambda r_0} = \frac{4\pi V_n x_i}{\lambda r_0} \text{ is circular Doppler frequency}$$

in the center of the observed from i -th point signal object ($t = 0$), $x_i = V_n t$,

$$\varphi_i = \varphi_{oi} - 2\pi V_n^2 t_i^2 / \lambda r_0 = \text{const} \quad V_n \text{ is ground speed.}$$

The reference function of the signal (4) is written as

$$\hat{h}_{m_0}(t) = H(t) \exp(j\alpha t^2), \quad (5)$$

where $H(t)$ is envelope of the reference function on the synthesis interval.

The method is called ‘‘harmonic analysis’’, since the multiplication of signals (4) by the reference function (5) corresponds to their linear-frequency (LFM) demodulation and for their isolation from the mixture with noise $\hat{\xi}_{mi}(t)$ harmonic analysis is used. Thus, the totality of responses to accurate reflectors can be obtained for the m -th strip by taking the Fourier transform of the products (4) and (5).

Returning to the discrete time, to represent the line of the radar signal, it is necessary to take the module of the discrete Fourier transform (DFT)

$$\hat{e}(m, k) = \left| \sum_{n=0}^{N_c-1} \hat{\xi}(m, n) \hat{h}_0(m, n) \exp(-j2\pi nk / N_c) \right|, \quad (6)$$

where $m = 0, 1, \dots, N_r - 1$; $k = 0, 1, \dots, N_c - 1$, N_r and N_c are sizes of SAR image.

Fig. 2a and Fig. 2b show examples of point small-sized object (a) and an extended distributed object (b) formation on the radar image using the method of harmonic analysis with following parameters $\lambda = 10^{-2} m$, $V_n = 200 m/s$, $\tau_u = 10^{-7} s$ and signal to noise (signal / background) ratio $q = 10$.

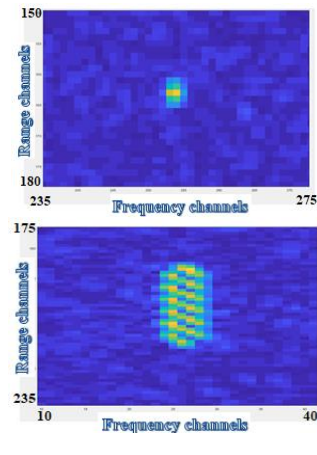


Fig. 2. Imitation of a point (a) and an extended (b) object on a radar image.

An analysis of Fig. 2 shows that even with the proposed modeling method, a point object on a radar image is represented by several points. This is due to the model of formation of such an image, one of the stages of the implementation of which is the use of DFT.

V. DETECTION AND RECOGNITION OF OBJECTS ON SAR IMAGES

A mixture of signals from the object (if it is present, otherwise its component can be taken equal to zero) and the background with noise is a total signal at the detector input

$$\hat{\xi}(m, k) = \hat{s}_\phi(m, k) + \hat{s}_o(m, k) + \hat{n}(m, k). \quad (8)$$

To detect useful signal in this case, it is also possible to use the classic comparison of the likelihood ratio with the threshold h , found from the Neyman-Pearson test, which provides a given probability of false alarm

$$l[\dot{\xi}(r, x)] = \frac{p_1(\dot{\xi}) \geq h \rightarrow H_1}{p_0(\dot{\xi}) < h \rightarrow H_0} \quad (9)$$

Here H_1 is hypothesis of the presence of a signal from an object, H_0 is hypothesis of the absence of a signal from the object. Expression (9) can be used in the case of complete a priori certainty. In the case of using uncertain parameters, the likelihood ratio is determined to within finite aggregates of undefined parameters λ_1 and λ_0 . Then equation (9) can be written in the form

$$l[\dot{\xi} / \lambda_0, \lambda_1] = \frac{p_1(\dot{\xi} / \lambda_1) \geq h \rightarrow H_1}{p_0(\dot{\xi} / \lambda_0) < h \rightarrow H_0} \quad (10)$$

where λ_0 and λ_1 are sets of informational and non-informational unknown distribution parameters $p_0(\dot{\xi})$ and $p_1(\dot{\xi})$ under hypotheses H_0 and H_1 .

The likelihood functions in (10) can be found with the known parameters of observation noise

$$p_1[\dot{\xi}(m, k / \lambda_1)] = k_n \exp \left\{ -\frac{1}{N_0} \sum_{m=0}^{N_1-1} \sum_{k=0}^{N_1-1} \left| \dot{\xi}(m, k / \lambda_1) - \dot{s}_o - \dot{s}_\phi(r, x) \right|^2 \right\}, \quad (11)$$

$$p_0[\dot{\xi}(m, k / \lambda_0)] = k_n \exp \left\{ -\frac{1}{N_0} \sum_{m=0}^{N_1-1} \sum_{k=0}^{N_1-1} \left| \dot{\xi}(m, k / \lambda_0) - \dot{s}_\phi(r, x) \right|^2 \right\},$$

where k_n is normalization factor, N_0 is spectral density of observation noise.

Fig. 3-5 show the detection characteristics. Here P_d is a probability of the correct detection. Fig. 3 presents the dependence of the correct detection on the ratio of the signal level to the background level for different numbers of accumulated frames, Fig. 4 shows the dependence of the probability of correct detection on the number of accumulated frames, Fig. 5 shows the dependence of the probability of correct detection on the threshold value. In all modeling and detection processes the probability of false alarm is $P_f = 10^{-3}$.

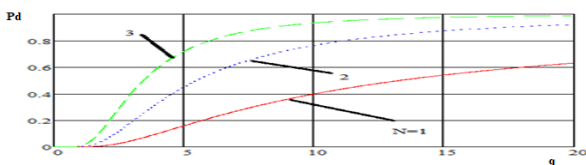


Fig. 3. Detection efficiency based on signal to noise ratio.

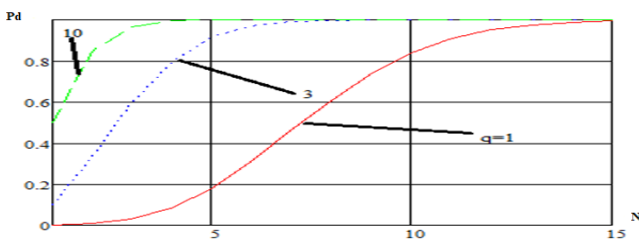


Fig. 4. Detection efficiency depending on the number of frames accumulated.

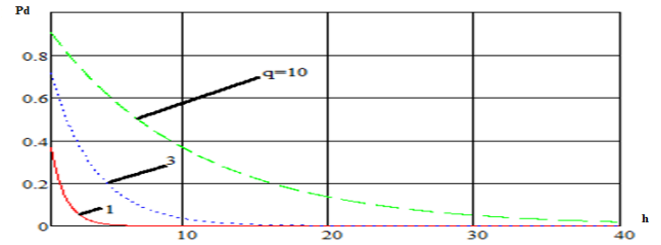


Fig. 5. Detection efficiency depending on threshold.

An analysis of the curves in the graphs of Fig. 3–5 shows that the best detection characteristics are achieved under conditions of accumulation of several information frames. It is also should be noted that at $N = 5$, if $q > 1$, good correct detection probabilities are achieved. It is also seen that for small q it is recommended to carefully choose the threshold, since with its increase the detection efficiency drops sharply.

Finally, based on detection results objects can be further recognized. For this, the correlation with the known pattern is considered in the detected area and the object for which it made the highest value is selected. Estimation for calculating the correlation is as follows

$$R_i = \sum_{m=0}^{N_r-1} \sum_{k=0}^{N_c-1} (\dot{\xi}(m, k) - \dot{s}_\phi) \dot{s}_{oi} \quad (12)$$

Thus, the characteristics of the detection of small objects on the radar are considered and an algorithm for recognizing such objects is proposed.

VI. CONCLUSION

The article discusses the main features of the formation of radar data and the principle of operation of a radar of SAR type. It is shown how to generate radar images using the harmonic analysis method. In addition, characteristics of the detection efficiency of small objects are obtained. It was revealed that with the probability of false alarm $P_f = 10^{-3}$ it is possible to get good detection results ($P_d > 0.9$) if at least 3 frames of SAR images is accumulated and the ratio of the signal level to the background level $q \geq 10$.

ACKNOWLEDGMENT

This work was funded by the RFBR Grant, Project No. 19-29-09048.

REFERENCES

- [1] K.K. Vasiliev, V.E. Dementiev and N.A. Andriyanov, "Filtration and restoration of satellite images using doubly stochastic random fields," CEUR Workshop Proceedings, vol. 1814, pp. 10-20, 2017.
- [2] N.A. Andriyanov and V.E. Dement'ev, "Application of mixed models of random fields for the segmentation of satellite images," CEUR Workshop Proceedings, vol. 2210, pp. 219-226, 2018.
- [3] K. Vasiliev, V. Dementiev, N. Andriyanov, "Representation and processing of multispectral satellite images and sequences," Procedia Computer Science, vol. 126, pp. 49-58, 2018. DOI: 10.1016/j.procs.2018.07.208.
- [4] N.A. Andriyanov and K.K. Vasiliev, "Optimal filtering of multidimensional random fields generated by autoregressions with multiple roots of characteristic equations," CEUR Workshop Proceedings, vol. 2391, pp. 72-78, 2019. DOI: 10.18287/1613-0073-2019-2391-72-78.

- [5] A.S. Shirokanev, D.V. Kirsh, N.Yu. Ilyasova and A.V. Kupriyanov, "Investigation of algorithms for coagulate arrangement in fundus images," *Computer Optics*, vol. 42, no. 4, pp. 712-721, 2018. DOI: 10.18287/2412-6179-2018-42-4-712-721.
- [6] N.Yu. Ilyasova, A.S. Shirokanev and N.S. Demin, "Analysis of Convolutional Neural Network for Fundus Image Segmentation," *Journal of Physics: Conference Series*, vol. 1438, pp. 1-7, 2019.
- [7] N.Yu. Ilyasova, A.S. Shirokanev, A.V. Kupriyanov, R.A. Paringer, D.V. Kirsh and V.A. Soifer, "Methods of Intellectual Analysis in Medical Diagnostic Tasks Using Smart Feature Selection," *Pattern Recognition and Image Analysis*, vol. 28, no. 4, pp. 637-645, 2018.
- [8] G.S. Kondratenkov and A.Yu. Frolov, "Radio vision. Earth remote sensing radar systems. Textbook for universities," M.: Radio Engineering, 2005, 368 p.
- [9] L.A. Shkolny, "Aerial reconnaissance radar systems, decoding of radar images: a textbook for cadets of the VVIA named after professor N.E. Zhukovsky," M.: VVIA named after prof. N.E. Zhukovsky, 2008, 531 p.
- [10] L.G. Dorosinsky, "Optimal processing of radar images formed in SAR: monograph," M.: Publishing House of the Academy of Natural Sciences, 2017, 212 p.
- [11] V.G. Kobernichenko, O.Yu. Ivanov and A.V. Sosnovsky, "Processing of radar data of remote sensing of the Earth," Yekaterinburg: Publishing House Ural. University, 2013, 64 p.
- [12] A.A. Morozov, O.S. Sushkova, "Development of Agent Logic Programming Means for Heterogeneous Multichannel Intelligent Visual Surveillance," *Advances in Artificial Intelligence: 16th Ibero-American Conference on AI, IBERAMIA*, Trujillo, Peru, November 13-16, Proceedings, vol. 11238, pp. 29-41, 2018. DOI: 10.1007/978-3-030-03928-8_3.
- [13] D.A. Zherdev, V.A. Procudin, E.Y. Minaev and V.A. Fursov, "HPC implementation of radar images modelling method using CUDA," *Journal of Physics: Conference Series*, vol. 1096, 012083, 2018. DOI: 10.1088/17426596/1096/1/012083.
- [14] V.A. Fursov, D.A. Zherdev and N.L. Kazanskiy, "Support subspaces method for synthetic aperture radar automatic target recognition," *Int. J. Adv. Robot. Systems*, vol. 13, no. 5, pp. 1-11, 2016. DOI: 10.1177/1729881416664848.
- [15] D.A. Zherdev, E.Y. Minaev, V.V. Procudin and V.A. Fursov, "Object recognition using real and modelled SAR images," *Procedia Engineering*, vol. 201, pp. 503-510, 2017. DOI: 10.1016/j.proeng.2017.09.473.
- [16] N.L. Kazanskiy, V.A. Fursov, E.Y. Minaev and D.A. Zherdev, "Radar image modeling and recognition," *Proc. SPIE*, vol. 11516, 115161J, 2020. DOI: 10.1117/12.2566467.